Article

Cell Reports

Phosphorylation and Ubiquitination Regulate Protein Phosphatase 5 Activity and Its Prosurvival Role in Kidney Cancer

Graphical Abstract

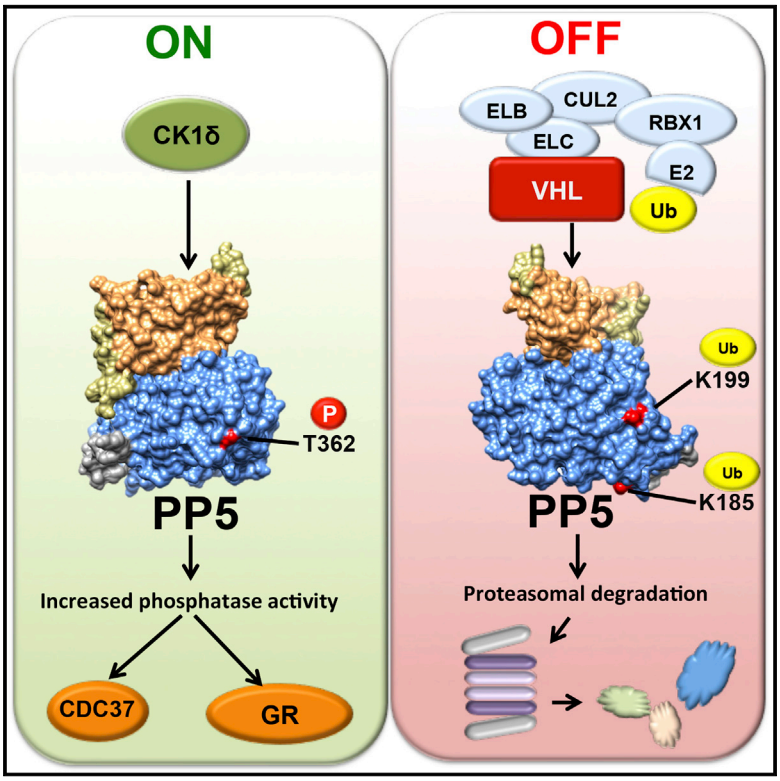

Highlights

- Casein kinase 1δ (CK1δ) phosphorylates T362 in the catalytic domain of PP5
- Phosphorylation activates and enhances the phosphatase activity of PP5
- Von Hippel-Lindau protein (VHL) multi-monoubiquitinates PP5 on K185 and K199
- PP5 downregulation in *VHL*-null clear cell renal cell carcinoma causes apoptosis

Authors

Natela Dushukyan, Diana M. Dunn, Rebecca A. Sager, ..., Gennady Bratslavsky, Dimitra Bourboulia, Mehdi Mollapour

Correspondence

mollapom@upstate.edu

In Brief

Dushukyan et al. show that casein kinase 1δ phosphorylates and activates protein phosphatase 5 (PP5), whereas von Hippel-Lindau protein (VHL) ubiquitinates and degrades PP5 in the proteasome. Kidney cancer cells with mutations and inactivation of *VHL* have elevated levels of PP5. Downregulation of PP5 causes apoptosis, demonstrating a prosurvival function for PP5 in kidney cancer.

Dushukyan et al., 2017, Cell Reports *21*, 1883–1895
November 14, 2017
https://doi.org/10.1016/j.celrep.2017.10.074

Cell Reports
Article

Phosphorylation and Ubiquitination Regulate Protein Phosphatase 5 Activity and Its Prosurvival Role in Kidney Cancer

Natela Dushukyan,[1,2,3,8] Diana M. Dunn,[1,2,3,8] Rebecca A. Sager,[1,2,3] Mark R. Woodford,[1,2] David R. Loiselle,[4] Michael Daneshvar,[1,2] Alexander J. Baker-Williams,[1,2,3] John D. Chisholm,[5] Andrew W. Truman,[6] Cara K. Vaughan,[7] Timothy A. Haystead,[4] Gennady Bratslavsky,[1,2] Dimitra Bourboulia,[1,2,3] and Mehdi Mollapour[1,2,3,9,*]
[1]Department of Urology
[2]Upstate Cancer Center
[3]Department of Biochemistry and Molecular Biology
SUNY Upstate Medical University, 750 E. Adams St., Syracuse, NY 13210, USA
[4]Department of Pharmacology and Cancer Biology, Duke University Medical Center, Durham, NC 27710, USA
[5]Department of Chemistry, Syracuse University, 1-014 Center for Science and Technology, Syracuse, NY 13244, USA
[6]Department of Biological Sciences, University of North Carolina at Charlotte, Charlotte, NC 28223, USA
[7]Institute of Structural and Molecular Biology, University College London and Birkbeck College, Biological Sciences, Malet Street, London WC1E 7HX, UK
[8]These authors contributed equally
[9]Lead Contact
*Correspondence: mollapom@upstate.edu
https://doi.org/10.1016/j.celrep.2017.10.074

SUMMARY

The serine/threonine protein phosphatase 5 (PP5) regulates multiple cellular signaling networks. A number of cellular factors, including heat shock protein 90 (Hsp90), promote the activation of PP5. However, it is unclear whether post-translational modifications also influence PP5 phosphatase activity. Here, we show an "on/off switch" mechanism for PP5 regulation. The casein kinase 1δ (CK1δ) phosphorylates T362 in the catalytic domain of PP5, which activates and enhances phosphatase activity independent of Hsp90. Overexpression of the phosphomimetic T362E-PP5 mutant hyper-dephosphorylates substrates such as the co-chaperone Cdc37 and glucocorticoid receptor in cells. Our proteomic approach revealed that the tumor suppressor von Hippel-Lindau protein (VHL) interacts with and ubiquitinates K185/K199-PP5 for proteasomal degradation in a hypoxia- and prolyl-hydroxylation-independent manner. Finally, *VHL*-deficient clear cell renal cell carcinoma (ccRCC) cell lines and patient tumors exhibit elevated PP5 levels. Downregulation of PP5 causes ccRCC cells to undergo apoptosis, suggesting a prosurvival role for PP5 in kidney cancer.

INTRODUCTION

The serine/threonine protein phosphatase 5 (PP5) belongs to the phosphoprotein phosphatase (PPP) family. Unlike other phosphatases within this family, PP5 is encoded by a single gene, and its regulatory and catalytic domains are all contained within the same polypeptide (Shi, 2009). Recently, a positive correlation between PP5 expression levels and breast cancer metastasis has been identified (Golden et al., 2008a), indicating that PP5 may act as an oncogene during carcinogenesis. Recent work has also shown the importance of PP5 in colorectal cancer cell growth (Wang et al., 2015).

PP5 generally has low basal activity, because the tetratricopeptide repeat (TPR) motif at its N terminus interacts with the αJ helix in the C terminus. This prevents substrates from entering the active site of PP5 (Cliff et al., 2006; Haslbeck et al., 2015a; Kang et al., 2001; Ramsey and Chinkers, 2002; Yang et al., 2005). Activation of PP5 depends on binding of its TPR domain to the molecular chaperone heat shock protein 90 (Hsp90) and client substrates. Other cellular factors such as polyunsaturated fatty acids also activate PP5 (Chatterjee et al., 2010; Ramsey and Chinkers, 2002; Yang et al., 2005).

The majority of PP5 substrates are in complex with Hsp90 and include the glucocorticoid receptor (GR), tumor suppressor p53, and the co-chaperone Cdc37 (Vaughan et al., 2008; Zuo et al., 1998, 1999). PP5 also functions as a co-chaperone of Hsp90 (Haslbeck et al., 2015b; Vaughan et al., 2008; Wandinger et al., 2006; Xu et al., 2012), and its dephosphorylation of Cdc37 in complex with Hsp90 activates kinase clients. Hsp90 and its co-chaperones are subject to post-translational modifications (PTMs) (Mayer and Le Breton, 2015; Walton-Diaz et al., 2013; Woodford et al., 2016a). However, it is unclear whether PP5 is also subject to any PTMs and how this impacts its phosphatase activity in cells. In this study, we found that CK1δ phosphorylates T362 in the catalytic domain of PP5, which is involved in its activation and hyperactivity, independent of Hsp90 binding. We also found that the tumor suppressor von Hippel-Lindau protein (VHL) targets K185/K199 for ubiquitination and proteasomal degradation of PP5 in a hypoxia-independent manner. Mutation and

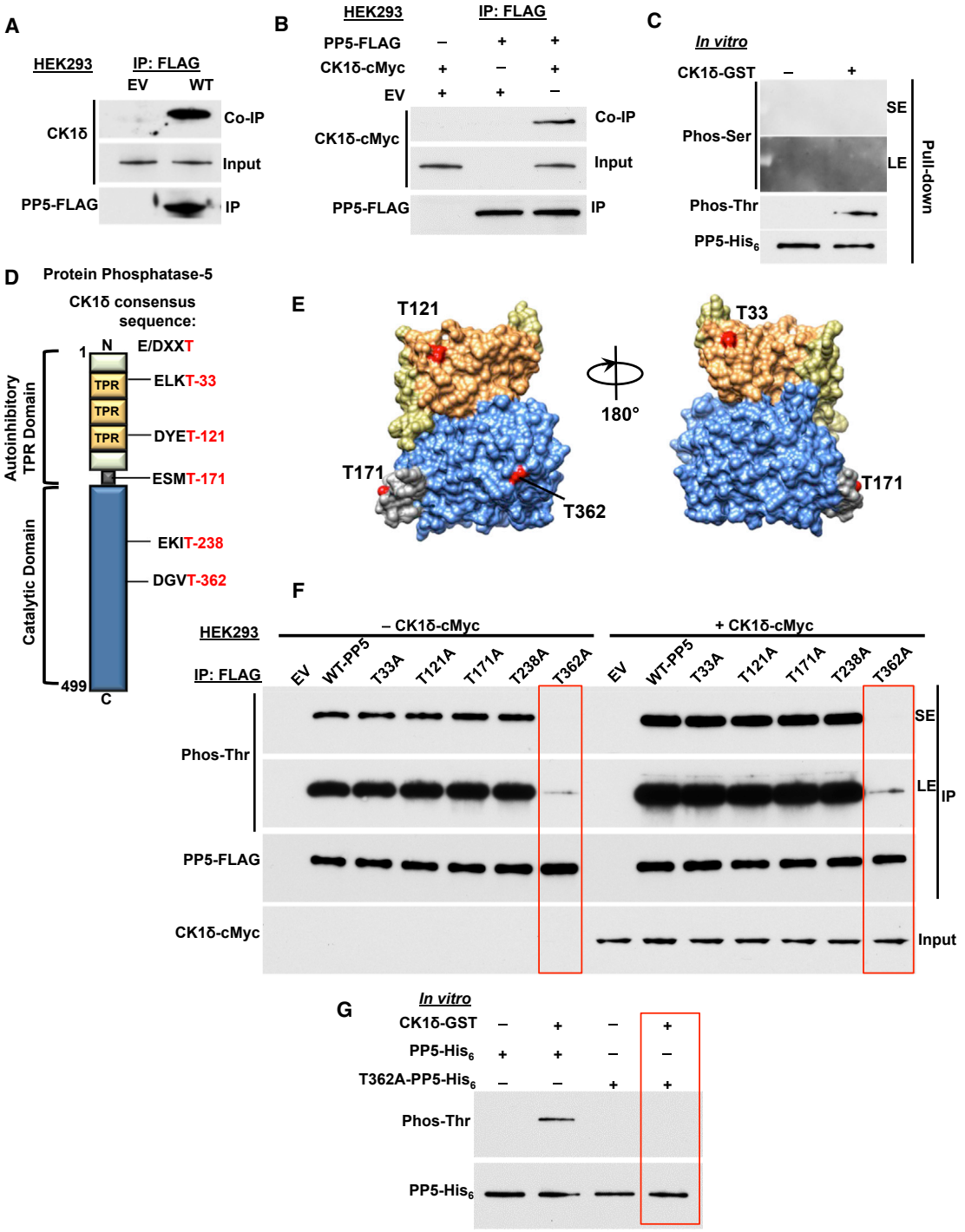

Figure 1. CK1δ Phosphorylates T362-PP5

(A) Empty vector (EV) or PP5-FLAG plasmids were transiently expressed and immunoprecipitated (IP) from HEK293 cells. Co-immunoprecipitation (Co-IP) of endogenous CK1δ was examined by immunoblotting. Empty vector was used as a control.

(B) PP5-FLAG and CK1δ-cMyc were transiently co-expressed in HEK293 cells. PP5-FLAG was IP and Co-IP of CK1δ-cMyc was assessed by immunoblotting. Empty vector was used as a control.

(C) Recombinant PP5-His6 was used in an *in vitro* kinase assay. CK1δ-GST phosphorylates only threonine residues on PP5-His6. Phosphorylation was examined by immunoblotting with anti-phosphoserine or phosphothreonine antibodies. SE (short exposure) and LE (long exposure) of the radiographic film.

(D) Schematic representation of PP5 with highlighted CK1δ consensus sequence E/DXXT.

(legend continued on next page)

inactivation of VHL is associated with clear cell renal cell carcinoma (ccRCC) (Cancer Genome Atlas Research Network, 2013). In the absence of VHL, PP5 was upregulated and hyperphosphorylated in ccRCC cells. Small interfering RNA (siRNA)-mediated silencing of PP5 induced apoptosis in VHL-null ccRCC, suggesting a prosurvival role for PP5 in these cells.

RESULTS

CK1δ Phosphorylates T362 in the Catalytic Domain of PP5

Previous work has shown that PP5 interacts with casein kinase 1 (CK1) (Partch et al., 2006). We used this information and showed that in yeast, Hrr25, the homolog of mammalian serine/threonine kinase casein kinase 1 δ (CK1δ), phosphorylates Ppt1 (yeast PP5) on both serine and threonine residues (Figure S1A). This was achieved by co-expressing C-terminally His_6-tagged Ppt1 under its native promoter and C-terminally cMyc-tagged Hrr25 under the galactose-inducible promoter of *GAL1* in yeast. Threonine and serine phosphorylation of Ppt1-His_6 was detectable by immunoblotting using pan-anti-phosphothreonine-P6623 and anti-phosphoserine-P5754 (Sigma-Aldrich) antibodies (Figure S1A). Growing yeast cells in galactose (i.e., overexpressing Hrr25-cMyc) led to hyperphosphorylation of Ppt1 on both threonine and serine sites (Figure S1A). We next asked whether similar phenomena also occur with human CK1δ and human PP5. N-terminal FLAG-tagged PP5 (PP5-FLAG) was transiently expressed in HEK293 cells. Using anti-FLAG M2 affinity gel, PP5-FLAG was immunoprecipitated, and co-immunoprecipitation of CK1δ was observed by immunoblotting (Figure 1A). A similar experiment was also conducted by transiently co-transfecting HEK293 cells with PP5-FLAG and N-terminally cMyc-tagged CK1δ. Immunoprecipitation of PP5-FLAG led to co-immunoprecipitation of CK1δ-cMyc (Figure 1B). These data show that CK1δ interacts with PP5.

Our previous work has shown that PP5-mediated dephosphorylation of the co-chaperone Cdc37 is essential for activation of the kinase clients of Hsp90 (Vaughan et al., 2008). We first established whether CK1δ is an Hsp90 client by treating HEK293 cells with 1 μM of the Hsp90 inhibitor ganetespib (GB) over time. This did not impact the stability of CK1δ (Figure S1B); therefore, it is unlikely that CK1δ is a client of Hsp90. We next examined whether CK1δ directly phosphorylates PP5 in an *in vitro* kinase assay. Bacterially expressed and purified PP5-His_6 was bound to Ni-NTA agarose and then incubated with active CK1δ-glutathione S-transferase (GST). Using immunoblotting and anti-phosphothreonine P6623 (Sigma-Aldrich) antibody, it was possible to detect threonine phosphorylation of PP5 (Figure 1C). Unlike in yeast, CK1δ does not phosphorylate any serine sites on PP5 (Figure 1C). There are seven mammalian CK1 isoforms, but CK1δ and CK1ε display the highest homology (Schittek and Sinnberg, 2014). We repeated our *in vitro* kinase assay with PP5-His_6 and CK1ε-GST. Surprisingly, CK1ε did not phosphorylate PP5 on threonine or serine sites (Figure S1C).

Generally, the CK1 consensus phosphorylation site is S/Tp-X-X-<u>S/T</u>, where S/Tp refers to phospho-serine or phospho-threonine priming sites, X refers to any amino acid, and the underlined residues refer to the target site (Flotow et al., 1990). We did not identify any possible threonine phosphorylation site using this consensus motif in PP5. CK1 also phosphorylates a related unprimed site, D/E-X-X-<u>S/T</u>, where the underlined residues refer to the phosphorylated amino acid (Flotow et al., 1990). We identified five threonine residues within this CK1 consensus site (Figure 1D): T33, T121, T171, T238, and T362. With the exception of T238, all the identified threonine sites are located on the surface of PP5 (Figure 1E). These sites were individually mutated to non-phosphorylatable alanine in the PP5-FLAG construct and transiently co-expressed with or without CK1δ-cMyc in HEK293 cells. PP5-FLAG was then immunoprecipitated with anti-FLAG M2 affinity gel, and threonine phosphorylation was detected by immunoblotting using anti-phosphothreonine-P6623 (Sigma-Aldrich) antibody. Overexpression of CK1δ-cMyc increased threonine phosphorylation of wild-type PP5-FLAG and all non-phosphorylatable threonine mutants except T362A-PP5-FLAG (Figures 1F and S1D). The threonine phosphorylation of this mutant was significantly lower, even with overexpression of CK1δ-cMyc (Figures 1F and S1D), suggesting that T362 is phosphorylated by CK1δ. We obtained further evidence by carrying out an *in vitro* kinase assay with bacterially expressed and purified wild-type PP5-His_6 and the non-phosphorylatable mutant T362A-PP5-His_6. We were unable to detect threonine phosphorylation of this mutant by immunoblotting (Figure 1G), therefore confirming that CK1δ targets and phosphorylates only T362 in PP5.

T362 Phosphorylation Activates and Increases PP5 Activity Independent of Hsp90

To determine the impact of T362 phosphorylation on the activation and activity of PP5, we initially tested the ability of T362-PP5 phosphomutants to dephosphorylate para-nitrophenyl phosphate (pNPP), a small molecule commonly used for assaying nonspecific phosphatase activity (Oberoi et al., 2016). Our data showed that the bacterially expressed and purified wild-type-PP5-His_6 had basal phosphatase activity, and the addition of Hsp90α stimulated this activity (Figures S2A and S2B). Phosphomimetic T362E-PP5-His_6 or CK1δ mediated phosphorylation of

(E) Potential CK1δ-targeted threonine sites on PP5 are highlighted on the cartoon representation of the PP5 protein, which was modeled with UCSF Chimera software (PDB: 1WAO) and colored in red as in (D).

(F) PP5-threonine residues within the CK1δ consensus sequence were mutated individually to alanine (A), transiently expressed, and IP from HEK293 cells. Threonine phosphorylation was detected by immunoblotting with anti-phosphothreonine antibody. This experiment was repeated with co-transfection of CK1δ-cMyc with the phospho-PP5-FLAG mutants in HEK293 cells. PP5-FLAG and its mutants were isolated and threonine phosphorylation was assessed by immunoblotting with anti-phosphothreonine antibody. Short exposure (SE) and long exposure (LE) of the radiographic film.

(G) Recombinant PP5-His6 and T362A-PP5-His6 were used as substrates of CK1δ-GST in an *in vitro* kinase assay. Phosphorylation was assessed by immunoblotting with anti-phosphoserine or phosphothreonine antibodies.

See also Figure S1.

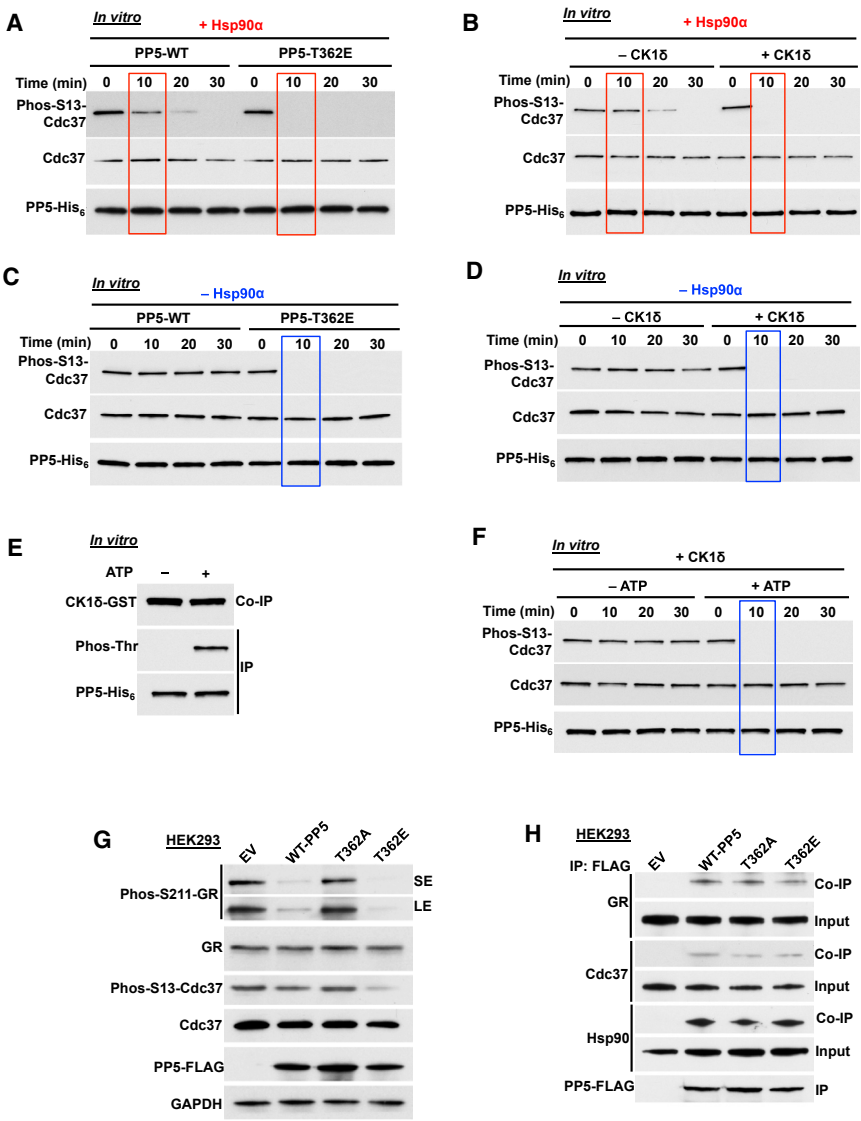

Figure 2. CK1δ-Mediated Phosphorylation of PP5 Activates and Increases the Rate of Phosphatase Activity

(A) Dephosphorylation of phospho-S13-Cdc37 with a recombinant wild-type PP5-His6 and phosphomimetic T362E-PP5-His6 in the presence of Hsp90α. The rate of Cdc37 dephosphorylation was assessed by immunoblotting with a phospho-specific S13-Cdc37 antibody over time (minutes).

(B) Recombinant wild-type PP5-His6 was phosphorylated by CK1δ *in vitro* and then used in the dephosphorylation of phospho-S13-Cdc37 *in vitro*. The assay was performed in the presence of Hsp90α. PP5 activity was assessed with immunoblotting using a phospho-specific S13-Cdc37 antibody over time (minutes).

(C) Dephosphorylation of phospho-S13-Cdc37 with recombinant wild-type PP5-His6 and phosphomimetic T362E-PP5-His6 was performed in the absence of Hsp90α. Activity was assessed with immunoblotting using a phospho-specific S13-Cdc37 antibody over time (minutes).

(D) Recombinant wild-type PP5-His6 was phosphorylated by CK1δ *in vitro* and then used in the dephosphorylation of phospho-S13-Cdc37 *in vitro* without Hsp90α. PP5 activity was assessed with immunoblotting using a phospho-specific S13-Cdc37 antibody over time (minutes).

(E) Recombinant PP5-His6 was used in an *in vitro* kinase assay with CK1δ-GST. PP5-His6 was immunoprecipitated (IP), and threonine phosphorylation of PP5 and co-immunoprecipitation (Co-IP) of CK1δ-GST were examined by immunoblotting with anti-phosphothreonine and anti-GST antibodies.

(F) Recombinant wild-type PP5-His6 was phosphorylated by CK1δ *in vitro* in the presence (+) or absence (–) of ATP. PP5-His6 proteins were then used in the dephosphorylation of phospho-S13-Cdc37 *in vitro* without Hsp90α. PP5 activity was assessed with immunoblotting using a phospho-specific S13-Cdc37 antibody over time (minutes).

(G) PP5-FLAG and T362-PP5 phosphomutants (T362A and T362E) were transiently transfected in HEK293 cells. Cdc37, phospho-S13-Cdc37, GR, and phospho-S211-GR protein levels were examined by immunoblotting. Empty vector (EV) was used as a control, and GAPDH was used as a loading control.

(H) Wild-type PP5-FLAG, non-phosphorylating T362A-PP5-FLAG, and phosphomimetic T362E-PP5-FLAG were transiently expressed and IP from HEK293 cells. Co-IP of GR, Cdc37, and Hsp90 was examined by immunoblotting.

See also Figure S2.

T362-PP5-His$_6$-stimulated PP5 activity in the absence of Hsp90α (Figures S2A and S2B). We repeated the same experiments but instead used non-phosphorylating T362A-PP5-His$_6$. This mutant had basal phosphatase activity similar to that of wild-type-PP5-His$_6$, suggesting that the mutation did not structurally affect PP5 activity. However, the addition of Hsp90α or CK1δ (in an attempt to phosphorylate T362A-PP5-His$_6$ *in vitro*) did not stimulate phosphatase activity (Figures S2A and S2B). We next used an *in vitro* dephosphorylation assay of phospho-S13-Cdc37, which is a bona fide substrate of PP5 (Vaughan et al., 2008). We first showed that the addition of Hsp90α to wild-type PP5 leads to complete dephosphorylation of phospho-S13-Cdc37 after 30 min (Figures 2A and 2B). However, the addition of Hsp90α to phosphomimetic T362E-PP5-His$_6$ (Figure 2A) or phospho-T362-PP5-His$_6$ (Figure 2B) led to dephosphorylation of Cdc37 after only 10 min. To determine whether activation of phospho-T362-PP5 is independent of Hsp90, we repeated the above experiment in the absence of Hsp90α. Our data revealed that wild-type PP5 is unable to dephosphorylate phospho-S13-Cdc37 in the absence of Hsp90α (Figures 2C and 2D). However, phosphomimetic T362E-PP5-His$_6$ (Figure 2C) or CK1δ mediated phosphorylation of T362-PP5 dephosphorylated (Figure 2D) phospho-S13-Cdc37 *in vitro*, even in the absence of Hsp90.

To ascertain whether CK1δ's interaction with PP5 caused an increase in its phosphatase activity, CK1δ was incubated with

PP5-His$_6$ in the presence and absence of ATP. CK1δ has the ability to interact with PP5-His$_6$ independent of ATP (Figure 2E). However, only CK1δ's incubation with PP5-His$_6$ in the presence of ATP (hence phosphorylation of PP5) is capable of activating PP5. This leads to dephosphorylation of PP5 substrate, (i.e., phospho-S13-Cdc37) (Figure 2F). Taken together, these *in vitro* data suggest that CK1δ-mediated phosphorylation of T362-PP5 causes activation and hyperactivity of PP5 phosphatase independent of binding to Hsp90.

To obtain further evidence for this observation, we overexpressed wild-type PP5-FLAG and the phosphomutants T362A and T362E in HEK293 cells. The dephosphorylation of PP5 substrates, phospho-S13-Cdc37 and phospho-S211-GR, was examined by immunoblotting. Overexpression of wild-type PP5-FLAG led to dephosphorylation of phospho-S13-Cdc37 and phospho-S211-GR (Figure 2G). This effect was enhanced by overexpression of phosphomimetic T362E-PP5-FLAG and unaffected (similar to the empty vector control) by T362A-PP5-FLAG, which is consistent with our *in vitro* data (Figure 2G). Finally, we confirmed that the interactions between the phospho-T362 mutants and Hsp90, Cdc37, and GR were not affected, and therefore, our observation is not due to a lack of interaction between PP5 mutants and the substrates (Figure 2H). Our *in vitro* and *in vivo* data here show that phosphorylation of T362-PP5 is involved in both the activation and hyperactivity of PP5. Furthermore, based on our *in vitro* results, CK1δ-mediated phosphorylation and activation of PP5 does not depend on binding to Hsp90.

VHL E3 Ligase Targets PP5 Independent of Hypoxia

To determine which binding partners of PP5 are involved in its regulation, we immunoprecipitated endogenous PP5 from HEK293 cells and identified its intracellular binding proteins by mass spectrometry (MS) analysis (see Experimental Procedures). Our interactome data identified VHL as a binding partner of PP5 (Table S1). VHL forms a multi-protein complex, VCB-Cul2 (VHL-elongin C-elongin B-cullin 2) and Rbx1, that acts as a ubiquitin ligase (E3) (Gossage et al., 2015; Kamura et al., 1999; Stebbins et al., 1999) and directs proteasome-dependent degradation of targeted proteins such as hypoxia-inducible factors (HIF1α or HIF2α) (Kamura et al., 2000). *VHL* is expressed as two known isoforms: VHL$_{30}$, with an apparent molecular weight of ~24–30 kDa (VHL$_{30}$), and VHL$_{19}$, which is ~19 kDa in size (Iliopoulos et al., 1995). Both isoforms appear to retain tumor-suppressor activity; however, VHL$_{30}$ is the commonly examined isoform. Here, we confirmed our interactome data by immunoprecipitating endogenous PP5 from HEK293 cells and detecting VHL$_{30}$ (Figure 3A). The reciprocal immunoprecipitation of the endogenous VHL$_{30}$ yielded PP5 (Figure 3B). Since VHL is the substrate recognition subunit of an E3 ubiquitin ligase, we overexpressed VHL$_{30}$ in the VHL-deficient ccRCC cell line 786-O and observed downregulation of endogenous PP5 by immunoblotting (Figure 3C). We next transiently transfected and expressed PP5-FLAG in the 786-O cell line. Using immunoprecipitation and immunoblotting, we were unable to detect PP5 ubiquitination in these cells (Figure 3D), even when treated with 50 nM of the proteasome inhibitor bortezomib (BZ) for 2 hr (Figure 3D). However, transient co-expression of PP5-FLAG and VHL$_{30}$-His$_6$ in 786-O cells for 16 hr and subsequent treatment with 50 nM BZ for 2 hr led to detection of distinct ubiquitination bands, suggesting multi-monoubiquitination of PP5-FLAG (Figure 3D). It is noteworthy that the anti-ubiquitin antibody used in these experiments (P4D1) recognizes both mono- and poly-ubiquitination. Taken together, these data suggest that VHL E3 ligase ubiquitinates and degrades PP5 in the proteasome.

Canonically, VHL substrates are recognized when hydroxylated by prolyl-hydroxylases (PHDs) at specific proline sites (Ivan et al., 2001; Jaakkola et al., 2001). To determine whether hydroxylation was essential for VHL-mediated ubiquitination of PP5, we first overexpressed three *EGLN* genes (*EGLN1*, *EGLN2*, and *EGLN3*) encoding for three isoforms of PHDs in HEK293 cells. Overexpression of these genes did not affect the endogenous PP5 protein levels but, as expected, markedly reduced HIF1α levels (Figure 3E). Treatment of HEK293 cells with the PHD inhibitor dimethyloxaloylglycine (DMOG) or the hypoxia mimetic deferoxamine (DFX) or $CoCl_2$ similarly did not affect PP5 protein levels (Figure S3A). As expected, these conditions all led to stabilization of HIF1α (Figure S3A). We obtained a similar result when we treated the Caki-1 ccRCC cell line (containing the wild-type *VHL* gene) with DMOG, DFX, or $CoCl_2$ (Figure S3B). Finally, we examined PP5 protein levels in Caki-1 cells cultured in normoxia and hypoxia (1% O_2, 5% CO_2, and 94% N_2). While HIF1α levels increased under hypoxia, PP5 levels were unchanged and similar to normoxia (Figure 3F). Finally, previous work has indicated that transcription of PP5 can be mediated by HIF1 (Zhou et al., 2004). We examined this possibility by using siRNA to silence *HIF1α* or *HIF2α* in HEK293 cells. Our results showed that neither HIF1α nor HIF2α is involved in the regulation of PP5 (Figure 3G). We conducted a similar experiment in 786-O ccRCC cells and silenced only *HIF2α* (HIF1α is downregulated in these cells). Our data also showed that HIF2α is not involved in PP5 expression in VHL-null 786-O cells (Figure S3C). These data indicate that VHL ubiquitinates PP5 independent of prolyl-hydroxylation and hypoxia.

VHL Ubiquitinates K185/K199-PP5

Based on the data available on PhosphoSitePlus (https://www.phosphosite.org), an online systems biology resource providing comprehensive information on PTMs of human proteins, we identified five ubiquitinated lysine sites (K32, K40, K185, K199, and K320) on PP5 (Figure 4A). All of these sites are located on the surface of the PP5 protein (Figure 4B). We individually mutated these lysine sites to a non-ubiquitinating arginine residue and transiently expressed them in HEK293 cells (Figure 4C). Ubiquitination of wild-type PP5 was detectable by immunoprecipitation and immunoblotting techniques (Figures 4C and S4A). However, ubiquitination of PP5 was significantly reduced in the K185R and K199R mutants (Figure 4C). Our data also showed that K185R and K199R-PP5-FLAG mutants were slightly more stable than the wild-type PP5-FLAG expressed in HEK293 cells (Figure S4B), whereas these mutants were expressed at the same levels as the wild-type PP5-FLAG in the VHL-null 786-O cells (Figure S4C).

We next created a K185R/K199R-PP5-FLAG double mutant and transiently expressed it in HEK293 cells. Ubiquitination of this mutant was undetectable by immunoprecipitation and

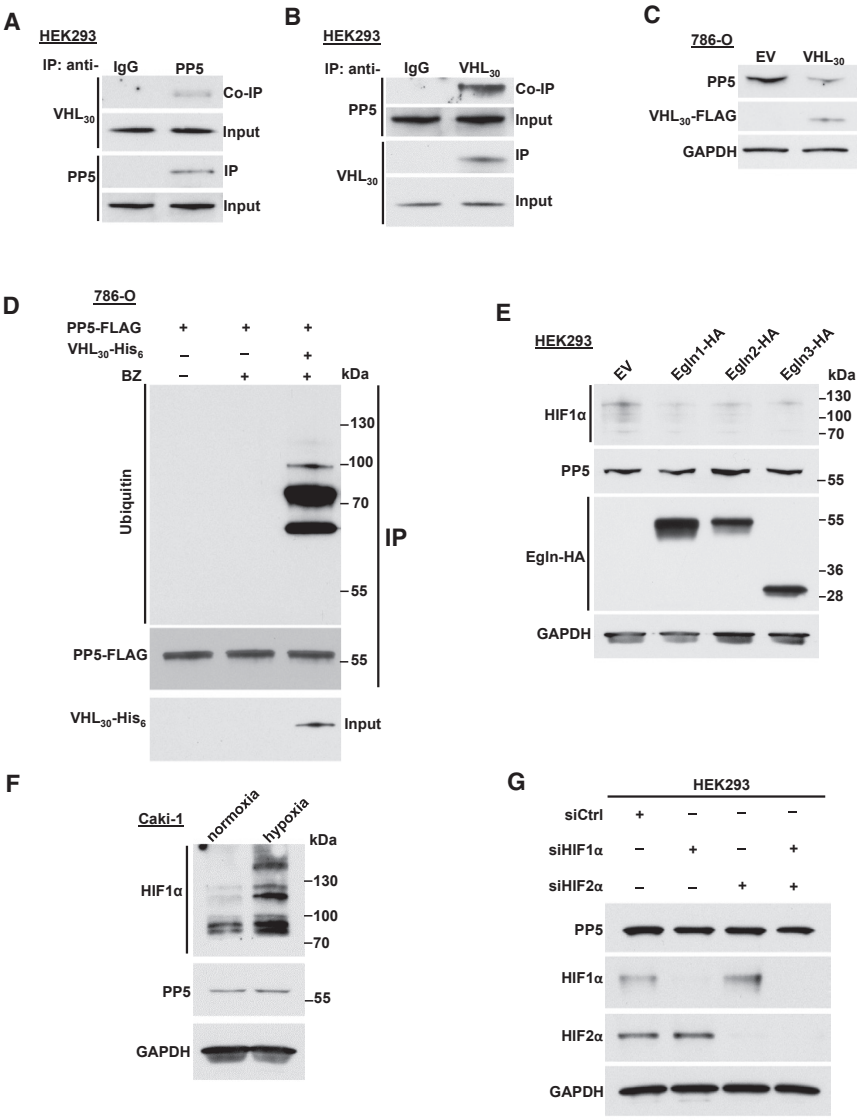

Figure 3. VHL E3 Ligase Ubiquitinates PP5 Independent of Hypoxia

(A) Endogenous PP5 was immunoprecipitated (IP) from HEK293 cells, and co-immunoprecipitation (Co-IP) of VHL30 was assessed by immunoblotting.

(B) Endogenous VHL30 was IP from HEK293 cells, and Co-IP of PP5 was examined by immunoblotting.

(C) VHL30-FLAG or empty vector (EV) was transiently overexpressed in 786-O cells and endogenous PP5 protein levels were assessed by immunoblotting. GAPDH was used as a loading control.

(D) 786-O cells transiently expressing PP5-FLAG were treated with or without 50 nM of the proteasome inhibitor bortezomib (BZ) for 2 hr. PP5-FLAG was also co-expressed with VHL30-His6 with additional treatment of 50 nM BZ for 2 hr. PP5-FLAG was IP, and its ubiquitination was assessed by immunoblotting.

(E) Egln1-HA, Egln2-HA, Egln3-HA, and empty vector (EV) pcDNA3.1 were transiently overexpressed in HEK293 cells. The expression of Egln1, 2, and 3, as well as PP5 and HIF1α, was assessed by immunoblotting with anti-HA, anti-PP5, and anti-HIF1α antibodies. GAPDH was used as a loading control.

(F) Caki-1 cells cultured in normoxia and hypoxia (1%O2, 5%CO2, 94%N2). PP5 and HIF1α protein levels were examined by immunoblotting using anti-PP5 and anti-HIF1α antibodies. GAPDH was used a loading control.

(G) HIF1α or HIF2α were silenced by small interfering RNA (siRNA) in HEK293 cells. HIF1α, HIF2α and PP5 protein levels were examined by immunoblotting using anti-HIF1α, anti-HIF2α and anti-PP5 antibodies. GAPDH was used as a loading control.

See also Figure S3.

immunoblotting experiments (Figures 4D and S4D). To determine whether VHL is responsible for ubiquitination of these sites, we used an *in vitro* ubiquitination assay kit (Millipore) with the VCB-Cul2 complex (Figure S4E). As mentioned earlier, VHL is part of a multi-protein complex, VCB-Cul2 and Rbx1, acting as a ubiquitin ligase (E3) and directing proteasome-dependent degradation of targeted proteins. Next, bacterially expressed and purified wild-type PP5-His$_6$ and K185R/K199R-PP5-His$_6$ double mutant were used in our *in vitro* ubiquitination assay. Our data show that recombinant wild-type PP5-His$_6$, but not the K185R/K199R-PP5-His$_6$ mutant, was subject to ubiquitination. Based on the immunoblots and the appearance of the bands, our data suggest that PP5 is subject to multi-monoubiquitination (Figure 4E), therefore suggesting that VHL targets K185/K199-PP5 for ubiquitination. To gain further evidence of VHL-mediated ubiquitination of K185/K199-PP5 in cells, we transiently co-expressed wild-type PP5-FLAG or K185R/K199R-PP5-FLAG with VHL$_{30}$-His$_6$ for 16 hr in VHL-null 786-O cells and then treated the cells with 50 nM BZ for an additional 2 hr. We were able to detect the ubiquitination of wild-type PP5, but not the K185R/K199R-PP5 double mutant (Figure 4F). The K185R-, K199R-PP5 single or double mutants interacted with the same affinity as wild-type PP5 to VHL$_{30}$ (Figure 4G). Therefore, the reduced ubiquitination of these mutants is not due to their inability to bind to VHL$_{30}$.

Taken together, our data show that VHL E3 ligase ubiquitinates K185 and K199 residues in PP5.

PP5 Downregulation Causes Apoptosis in VHL-Null ccRCC Cells

To gain further insight into the significance of PP5 stability and hyperactivity in ccRCC, we first examined PP5 protein levels in tumors and adjacent normal tissues from nine patients with ccRCC. Within 10 min of removal of tumors by radical or partial nephrectomy, tumors and adjacent normal tissues were dissected into 10-mm^3 pieces and stained with H&E (Figure 5A),

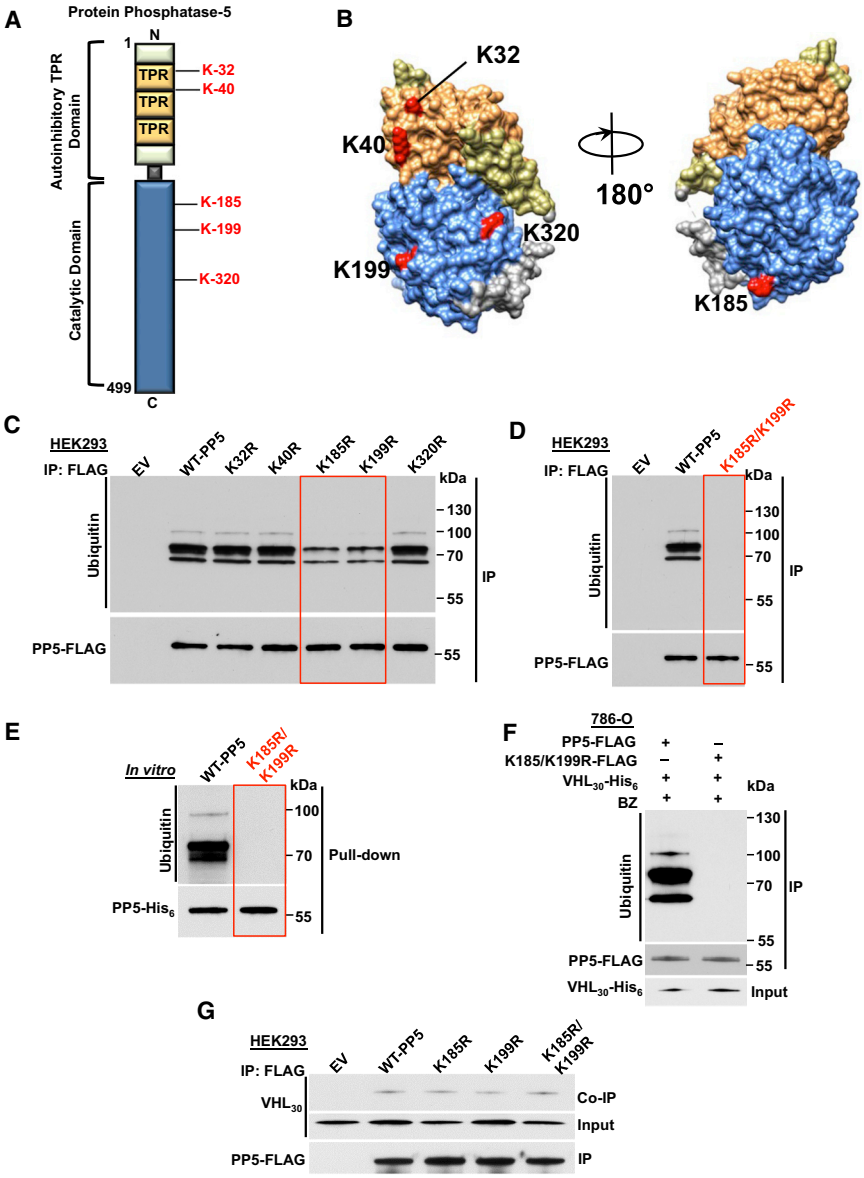

Figure 4. VHL-Mediated Ubiquitination and Proteasomal Degradation of K185/K199-PP5

(A) Schematic representation of PP5 highlighting the lysine residues possibly subject to VHL-mediated ubiquitination.

(B) Potential ubiquitinating lysine residues are highlighted in the cartoon representation of the PP5 protein, which was modeled with UCSF Chimera software (PDB: 1WAO) and colored in red as in Figure 1D.

(C) Wild-type PP5-FLAG and its potentially non-ubiquitinating lysine mutants were transiently expressed and immunoprecipitated (IP) from HEK293 cells. Ubiquitination of PP5 was examined by immunoblotting. Empty vector (EV) was used as a control.

(D) Wild-type PP5-FLAG and its non-ubiquitinating K185/K199R mutant were transiently expressed and IP from HEK293 cells. Ubiquitination of PP5 was examined by immunoblotting anti-ubiquitin antibody. Empty vector (EV) was used as a control.

(E) Recombinant PP5-His6 and K185/K199R double mutant were used in an *in vitro* ubiquitination assay with VCB-Cul2 (VHL30-elongin C-elongin B-cullin 2) and Rbx1, which acts as an ubiquitin-ligase (E3). Ubiquitination of PP5 was assessed with immunoblotting.

(F) PP5-FLAG or K185/K199R-PP5-FLAG double mutant was co-transfected with VHL30-His6 in 786-O cells and treated 16 hr later with 50 nM BZ for 2 hr. PP5-FLAG or K185/K199R-PP5-FLAG was IP, and ubiquitination was assessed by immunoblotting.

(G) PP5-FLAG, K185-PP5-FLAG, K199R-PP5-FLAG, K185/K199R-PP5-FLAG, and empty vector (EV) were individually and transiently expressed in HEK293 cells. They were IP, and their interactions with VHL30 were assessed in the Co-IP by immunoblotting.

See also Figure S4.

and protein was extracted (Figure 5B). Our data showed that VHL_{30} is absent in ccRCC tumors. Conversely PP5 and CK1δ were both upregulated in tumors compared with adjacent normal tissue (Figure 5B).

We confirmed this finding using established *VHL*-deficient (786-O and A-498) and *VHL*-containing (Caki-1) ccRCC cell lines. Our data showed that PP5 was upregulated in 786-O and A-498 cells compared to Caki-1 cells (Figure 5C). CK1δ levels displayed a similar expression pattern, while CK1ε levels were unchanged between VHL-deficient and VHL-containing ccRCC cell lines (Figures 5C and S5A). This pattern was consistent with dephosphorylation of the PP5 substrates Cdc37 and GR, which were both more dephosphorylated in 786-O and A-498 cells than in VHL-containing Caki-1 cells (Figure 5C). We next used siRNA to silence *PP5* in 786-O and Caki-1 cells and observed induction of the pro-apoptotic markers cleaved caspase-3 and cleaved-poly-ADP-ribose polymerase (PARP) only in VHL-null 786-O cells (Figure 5D). We also found that silencing of *PP5* in 786-O cells did not affect CK1δ protein levels (Figure S5B). Furthermore, siRNA silencing of *PP5* in A-498 cells (VHL-null cell line) also led to induction of the apoptotic markers cleaved caspase-3 and cleaved PARP (Figure 5E).

To evaluate the threonine phosphorylation status of PP5 in VHL-null cells, we immunoprecipitated endogenous PP5 from 786-O and Caki-1 cells and found that PP5 from VHL-null 786-O cells was hyperphosphorylated on threonine residues (Figure 5F). Because IC261 is a potent specific inhibitor of CK1δ/ε, we next examined whether pharmacologic inhibition of CK1δ reduces threonine phosphorylation of PP5. In 786-O cells treated or untreated with 2 μM IC261 for 16 hr, PP5 was immunoprecipitated and as expected, IC261 treatment led to a marked reduction of PP5 threonine phosphorylation but not serine phosphorylation (Figure 5G). Taken together, our data

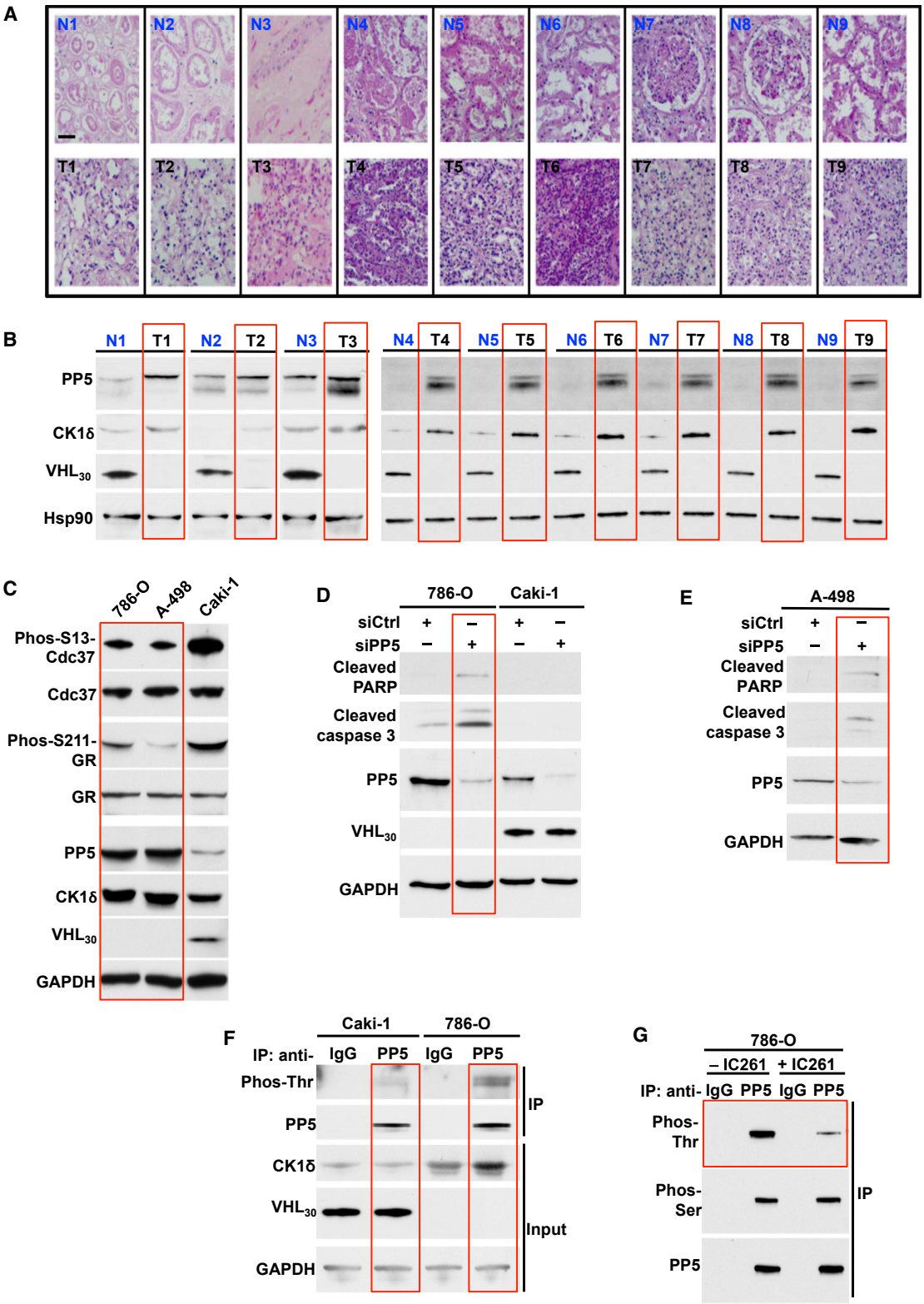

Figure 5. Downregulation of PP5 Induces Apoptosis in VHL-Deficient ccRCC Cells

(A) Clear cell renal cell carcinoma (ccRCC) tumors (T) and adjacent normal tissue (N) were stained with H&E. Scale bar represents 200 μm.

(B) Protein was extracted from tumors and adjacent normal tissue, and expression of PP5, CK1δ, VHL30, and Hsp90 was examined by immunoblotting. Hsp90 was used as a loading control.

(legend continued on next page)

show that PP5 is upregulated and phosphorylated by CK1δ in VHL-null ccRCC cells. Downregulation of *PP5* in VHL-null cells causes apoptosis.

PP5 Upregulation Provides a Prosurvival Mechanism in VHL-Null ccRCC Cells

We next examined whether pharmacologic inhibition of CK1δ causes apoptosis in VHL-null cells (A498 and 786-O). We used Caki-1 cells as a control, because this ccRCC cell line has the *VHL* gene. These cell lines were treated with different amounts of IC261, which is a potent specific inhibitor of CK1δ/ε. Increasing amounts of IC261 correlated with increased induction of the pro-apoptotic markers cleaved caspase-3 and cleaved PARP only in A498 and 786-O (VHL-null) cells (Figure 6A). Another hallmark of apoptosis is the loss of cell membrane integrity, which can be monitored by Annexin V/propidium iodide (AV/PI) staining. We treated A498, 786-O, and Caki-1 cells with 0.5 μM and 2.0 μM IC261 for 16 hr prior to analysis of apoptosis by AV/PI staining. Treatment of A498 and 786-O cells with 2.0 μM IC261 caused cells to progress through the AV+/PI− apoptotic quadrant (Figures 6B and S6A). However, this effect was not observed in Caki-1 cells after the same treatment with IC261 (Figures 6B and S6A). We next examined the effects of IC261 on proliferation of ccRCC cell lines. A498, 786-O, and Caki-1 cells were treated with different amounts of CK1δ inhibitor (IC261). After 72 hr, proliferation was measured by a 3-(4, 5-dimethylthiazolyl-2)-2, 5-diphenyltetrazolium bromide (MTT) assay. Our data revealed that 2.0 μM IC261 significantly inhibited the proliferation of A498 and 786-O cells compared to Caki-1 cells (Figure 6C). A hallmark of tumorigenic cells is anchorage-independent growth, which is measurable by soft agar assay. Treatment with 2.0 μM IC261 significantly reduced the anchorage-independent growth of A498 and 786-O cells compared to Caki-1 cells (Figures 6D and S6B).

Although treatment of VHL-null cells with IC261 caused apoptosis, it is unclear whether this effect was due to lack of PP5 phosphorylation and activity. We addressed this question by transiently expressing wild-type PP5-FLAG and its phospho-PP5 mutants T362A and T362E in 786-O cells. Treating cells expressing empty vector (EV) or non-phosphorylatable T362A-PP5-FLAG mutant with 2.0 μM IC261 led to induction of the pro-apoptotic markers cleaved caspase-3 and cleaved PARP. This effect was significantly reduced upon expression of wild-type PP5-FLAG and completely abrogated with the phosphomimetic T362E-PP5-FLAG mutant (Figure 6E). We further confirmed these data using an MTT assay. Our data showed that treatment of 786-O cells transiently expressing EV or non-phosphorylatable T362A-PP5-FLAG mutant with 2.0 μM IC261 caused a marked reduction in cell proliferation, whereas this effect was not observed in 786-O cells expressing wild-type PP5-FLAG and phosphomutant T362E-PP5 treated with 2.0 μM IC261 (Figures 6F and S6C).

Taken together, our findings show that pharmacologic inhibition of CK1δ causes apoptosis in ccRCC cells, and this effect is mediated by a lack of threonine phosphorylation of PP5 and reduced phosphatase activity.

DISCUSSION

PP5 plays a key role in the regulation of both hormone- and stress-induced signaling networks that allow cells to respond appropriately to genomic stress (Golden et al., 2008b). Structural work and *in-vitro*-based assays have shown that PP5 activity is promoted by a number of cellular factors, including the molecular chaperone Hsp90 and fatty acids, both of which release autoinhibition by interacting with the TPR domain of PP5 (Ramsey and Chinkers, 2002; Yang et al., 2005). In this study, we elucidated an alternative mechanism for activation and regulation of PP5 both *in vitro* and *in vivo*. Our data showed that the serine/threonine kinase CK1δ interacts with and phosphorylates T362 on PP5. This in turn activates PP5 independent of binding to Hsp90. We have also shown that CK1δ is not a client of Hsp90, because pharmacologic inhibition of Hsp90 did not affect the stability of CK1δ. Additionally, binding of CK1δ to PP5, without phosphorylation, is insufficient to activate PP5. Our cell-based assays have demonstrated that expression of non-phosphorylating T362A-PP5 did not dephosphorylate PP5 substrates such as GR and Cdc37, whereas overexpression of phosphomimetic T362E-PP5 had the opposite effect on those two substrates. Our findings clearly demonstrate that although phosphorylation of T362-PP5 does not affect the binding of PP5 to its substrates or even Hsp90, the phosphatase activity of PP5 is influenced by T362 phosphorylation (Figure 7).

What is the mechanism of phosphorylation-mediated PP5 activation? Threonine-362 is close to one of the six metal-coordinating sites, H352, but it is remote from the catalytic site. T362 is also at the center of an acidic patch located between D365, D364 and E416, E417. The latter residues are linked to the active site R400. Therefore, it is conceivable that phosphorylation or phosphomimetic mutation of T362 could either destabilize the domain as a whole or cause some local unfolding, possibly

(C) PP5, Cdc37, and phosphorylated S13-Cdc37, GR, phosphorylated S211-GR, CK1δ, and VHL30 proteins from the ccRCC cell lines 786-O, A-498 (VHL deficient), and Caki-1 (VHL containing) were assessed by immunoblotting. GAPDH was used as a loading control.

(D) PP5 was silenced by siRNA in 786-O and Caki-1 cells. siCtrl represents the non-targeting siRNA control. Induction of apoptotic markers shown by immunoblotting using anti-cleaved caspase-3 and cleaved PARP antibodies. GAPDH was used as a loading control.

(E) Targeted siRNA was used to silence PP5 in A498 cells. siCtrl represents the non-targeting siRNA control. Induction of apoptotic markers shown by immunoblotting using anti-cleaved caspase-3 and cleaved PARP antibodies. PP5 protein levels were also examined by immunoblotting. GAPDH was used as a control.

(F) PP5 was immunoprecipitated (IP) from ccRCC cell line (Caki-1 and 786-O) lysates using anti-PP5 antibody or immunoglobulin G (IgG) (control). Threonine phosphorylation of PP5 was assessed by immunoblotting with anti-phosphothreonine antibody. GAPDH was used as a loading control.

(G) PP5 was isolated from the lysates of 786-O cells treated with 2 μM IC261 for 16 hr using anti-PP5 or IgG (control) antibodies. Threonine phosphorylation of PP5 was examined by immunoblotting using anti-phosphothreonine antibody. Anti-phosphoserine antibody was used as a control.

See also Figure S5.

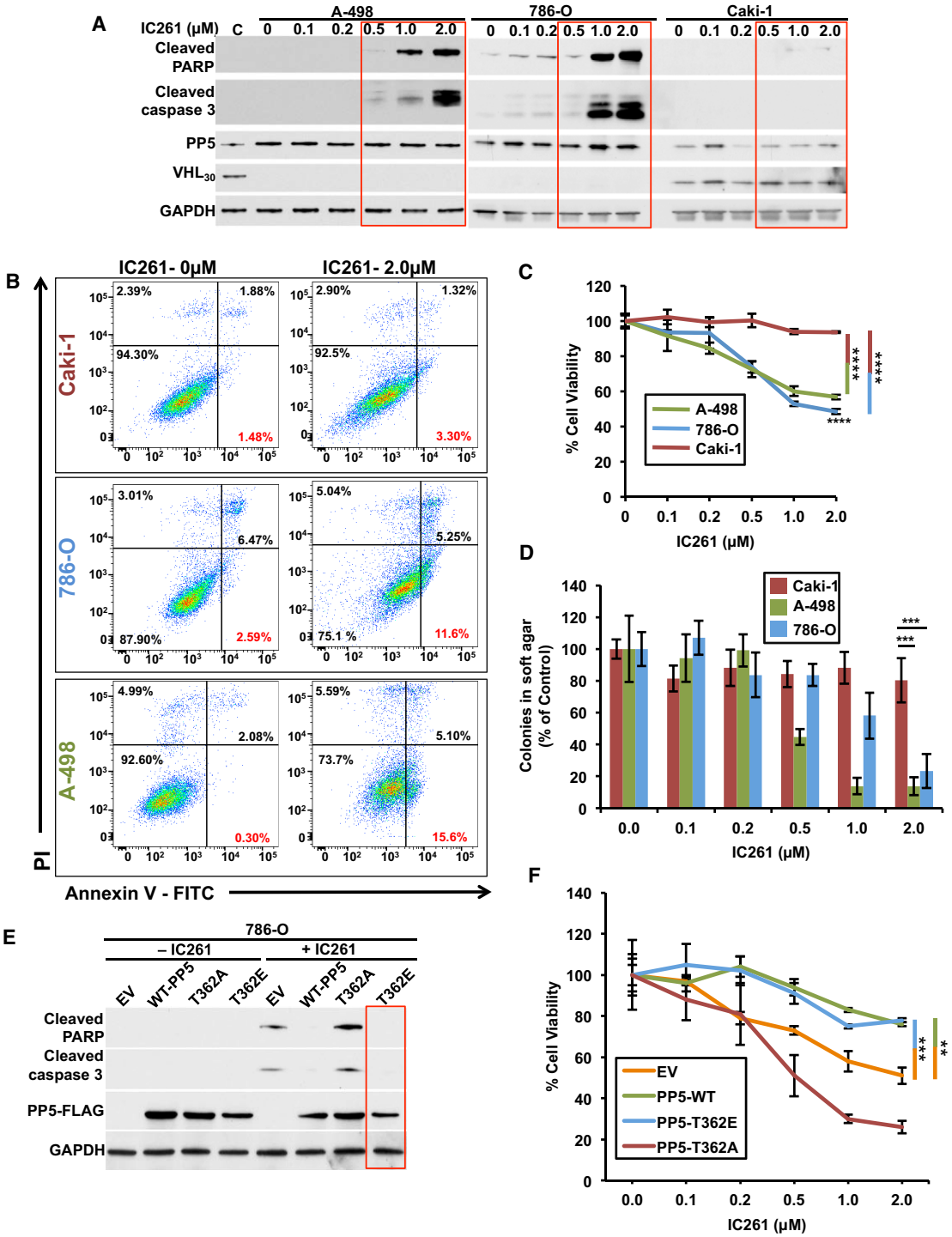

Figure 6. CK1δ Inhibition Induces Apoptosis and Reduced Proliferation in VHL-Null ccRCC Cells

(A) The ccRCC cell lines A498, 786-O, and Caki-1 were treated with the indicated amounts of the CK1δ inhibitor IC261 for 16 hr. Induction of apoptotic markers was assessed by immunoblotting using anti-cleaved caspase-3 and cleaved PARP antibodies. GAPDH was used as a loading control.

(B) AV/PI graphs of Caki-1, A498, and 786-O cells not treated (0 μM) or treated with 2 μM IC261 for 16 hr. The top left quadrants represent dead cells stained only with PI. The bottom right quadrants represent apoptotic cells stained with AV only. The top right quadrants represent cells stained with both PI and AV (secondary necrosis and late apoptosis). The percentage of each stained cell population is indicated. Dot plots shown are representative of one of three independent experiments.

(legend continued on next page)

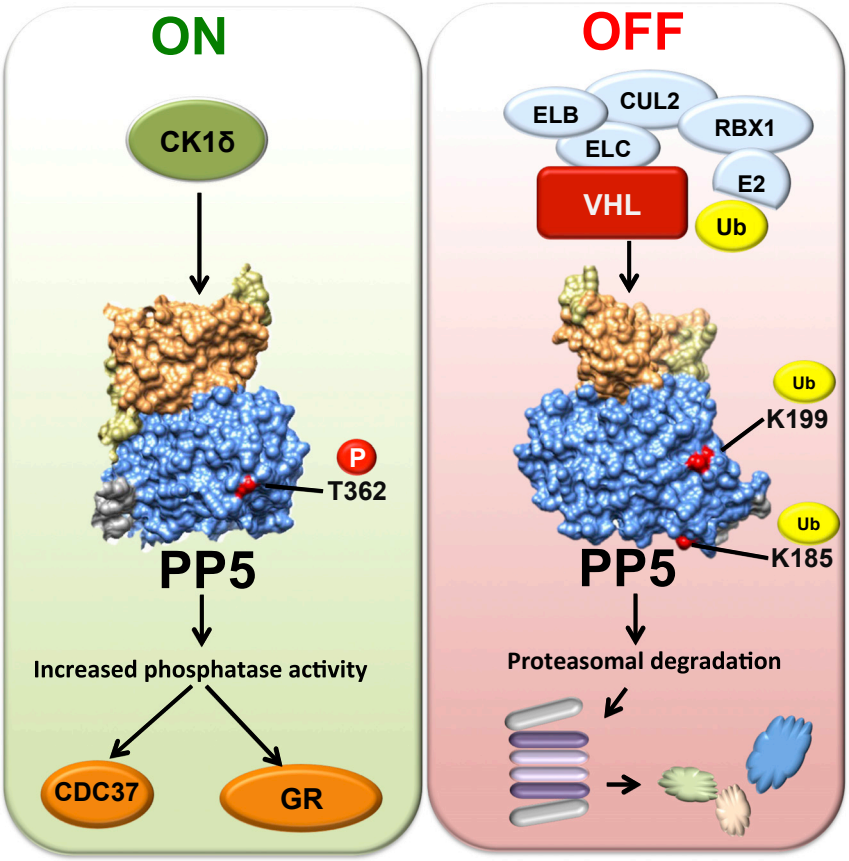

Figure 7. Post-translational Regulation of PP5
CK1δ-mediated phosphorylation of T362 in the catalytic domain of PP5 activates and enhances its phosphatase activity, therefore dephosphorylating its substrates, such as the co-chaperone Cdc37 and the steroid hormone receptor GR. VCB-Cul2 (VHL-elongin C-elongin B-cullin 2) and Rbx1 (E3 ubiquitin ligase) target and ubiquitinate K185 and K199 on PP5. This leads to proteasomal degradation of PP5.

allosterically "opening" the active site, therefore increasing the rate of phosphatase activity.

Our proteomic data also identified an interaction between the tumor suppressor VHL and PP5. VHL is an E3 ligase that canonically recognizes its substrates as part of an oxygen-dependent PHD reaction, with HIFα being its most-studied substrate (Clifford et al., 2001; Kondo et al., 2002; Maxwell et al., 1999). Our data revealed that PP5 is a hypoxia-independent target for VHL ubiquitination. We also showed that VHL ubiquitinates K185/K199-PP5 to target this phosphatase for proteasome-mediated degradation (Figure 7). Our finding of a hypoxia-independent function of VHL is not unusual; recent work has shown that VHL also directly multi-monoubiquitinates Aurora kinase A (AURKA) independent of oxygen or PHD activity (Hasanov et al., 2017).

Mutation and inactivation of VHL is associated with the most common type of kidney cancer, ccRCC (Cancer Genome Atlas Research Network, 2013; Gossage et al., 2015). We further demonstrated that inactivation of VHL in tumors or established cell lines leads to increased PP5 protein levels. This appeared to be independent of HIF1α or HIF2α. Our findings also provided a prosurvival role for PP5 in VHL-null kidney cancer cells. Downregulation of PP5 by siRNA activated apoptosis in ccRCC cells. This effect was apparent only in VHL-null ccRCC cells. We also showed that pharmacologic inhibition of CK1δ by IC261 leads to apoptosis and decreased proliferation of ccRCC cells. This effect was completely abrogated by overexpressing the phosphomimetic T362E-PP5 mutant in IC261-treated VHL-null ccRCC cells. Our findings therefore strongly suggest that the apoptotic effect of CK1δ inhibition is mediated by a lack of phosphorylation and thus inactivation of PP5 in ccRCC cells. It is worth noting that IC261 is also a potent inhibitor of CK1ε; however, CK1ε does not phosphorylate PP5. Although the apoptotic effect of IC261 may be the result of CK1ε inhibition, this possibility is highly unlikely, because treatment of 786-O cells overexpressing phosphomimetic T362E-PP5 with IC261 did not induce apoptosis.

Based on previous studies, there is circumstantial evidence suggesting that aberrant expression of PP5 may aid tumor development and progression (Golden et al., 2008a; Wang et al., 2015). Our study here also suggests that upregulation of PP5 is essential for ccRCC cell survival, but how is this achieved by PP5? Our previous work has shown that PP5-mediated dephosphorylation of the co-chaperone Cdc37 is essential for activation

(C) MTT assay of A498, 786-O, and Caki-1 cells treated with the indicated amounts of IC261. Errors bars represent the SD of three independent experiments (****$p < 0.0001$).
(D) Anchorage-independent growth of A498, 786-O, and Caki-1 cells treated with indicated amounts of IC261 in soft agar. Colony number was quantified. The errors bars represent the SD of three independent experiments (***$p < 0.0005$).
(E) Wild-type PP5-FLAG, non-phosphorylating T362A-PP5-FLAG, and phosphomimetic T362E-PP5-FLAG were transiently expressed in 786-O cells. Cells were then either not treated (−IC261) or treated (+IC261) with 2 μM IC261 for 16 hr, and induction of apoptotic markers was assessed by immunoblotting using anti-cleaved caspase-3 and cleaved PARP antibodies. GAPDH was used as a loading control.
(F) MTT assay of 786-O cells transiently expressing wild-type PP5-FLAG, T362A-PP5-FLAG, and T362E-PP5-FLAG and then treated with the indicated amounts of IC261. Errors bars represent the SD of three independent experiments (**$p < 0.005$; ***$p < 0.0005$).
See also Figure S6.

of the kinase client proteins of Hsp90 (Vaughan et al., 2008). Several of these clients, including vascular endothelial growth factor (VEGF) and platelet-derived growth factor (PDGF) receptors, as well as the mammalian target of rapamycin (mTOR), are important in ccRCC (Gossage et al., 2015; Linehan, 2012) and therefore potentially rely on the co-chaperone activity of PP5. Downregulation of PP5 in these cells appears to be detrimental for ccRCC cell survival, perhaps because of compromised function of these kinases. PP5 has been shown to be a negative regulator of the ASK1/MKK4/JNK signaling that promotes apoptosis (Zhou et al., 2004), and its overexpression, under hypoxia, in breast cancer has been shown to turn off this apoptotic signaling pathway. In contrast to a previous study (Zhou et al., 2004), we were unable to show HIF1 or HIF2 involvement in the regulation of PP5.

Further investigation is warranted to identify the exact signaling pathways dependent on PP5 function in VHL-null ccRCC cells and whether downregulation of PP5 activates the intrinsic or extrinsic apoptotic pathway. These findings could ultimately have therapeutic implications.

EXPERIMENTAL PROCEDURES

Plasmids, Yeast Strains, and Yeast Growth Media

Detailed methodologies, a list of primers (Table S2), and media conditions for both yeast and mammalian cells are provided in Supplemental Experimental Procedures.

Analysis of Human ccRCC Tumors

Tumor and adjacent normal tissues of patients with conventional ccRCC were obtained with written informed consent from the Department of Urology at SUNY Upstate Medical University and approved by the institutional review board. Because each patient's identity was kept confidential, information on gender and age was not available. At the time of radical or partial nephrectomy, which was done with <10 minutes of renal ischemia, ccRCC tumors were dissected into ~8 mm^3 pieces and protein was extracted and quantified as previously described in detail (Woodford et al., 2016b). The tissues were also stained with H&E and examined by a pathologist.

Protein Extraction, Immunoprecipitation, and Immunoblotting

Protein extraction from yeast, mammalian cells, and human tissues was carried out using methods previously described (Mollapour et al., 2010; Woodford et al., 2016b). Detailed methodology is provided in Supplemental Experimental Procedures.

In Vitro Cdc37 Dephosphorylation Assay

The rate of dephosphorylation of S13-Cdc37 by PP5 was monitored by mixing 5 μM purified phospho-S13-Cdc37 without or with 2.5 μM Hsp90α in a buffer containing 100 mM NaCl, 50 mM Tris (pH 7.5), 2 mM DTT, and 1 mM $MnCl_2$. The reaction was started by adding 0.25 μM PP5 (wild-type or phosphomutants or the CK1δ-mediated phosphorylated form), and samples were incubated at 30°C. Samples were taken every 10 min for SDS-PAGE analysis. The phosphorylation state of S13-Cdc37 was examined by immunoblotting using a phospho-Ser13-specific antibody (Abcam).

PP5 Activity Assay with pNPP

PP5 activity was assayed *in vitro* using a pNPP assay as previously described (Oberoi et al., 2016). Detailed methods are provided in Supplemental Experimental Procedures.

In Vitro Ubiquitination of PP5

Detailed methods for *in vitro* ubiquitination of PP5 are provided in Supplemental Experimental Procedures.

Annexin V/PI Apoptosis Analysis

Apoptosis was detected by Annexin V/PI immunostaining assay as described by the manufacturer (Bio-Rad/AbD Serotec). Detailed methods are provided in Supplemental Experimental Procedures.

MTT Assay

A498, 786-O, and Caki-1 cells were plated at 10,000 cells per well in 96-well plates. Cells were treated with 0.1, 0.2, 0.3, 0.5, 1.0, and 2.0 μM IC261. After 72 hr, an MTT assay was performed according to the manufacturer's protocol (BioVision, catalog number K302-500). Detailed methodology is described in Supplemental Experimental Procedures.

Soft Agar Colony-Formation Assay

Soft agar colony formation assay was performed similar to a previously described method (Borowicz et al., 2014). Detailed methodology can be found in Supplemental Experimental Procedures.

Quantification and Statistical Analysis

The data presented are representative of three biological replicates unless otherwise specified. Data were analyzed with an unpaired t test. Asterisks in the figures indicate significant differences (*$p < 0.05$; **$p < 0.005$; ***$p < 0.0005$; ****$p < 0.0001$). Error bars represent the SD for three independent experiments unless otherwise indicated.

SUPPLEMENTAL INFORMATION

Supplemental Information includes Supplemental Experimental Procedures, six figures, and three tables and can be found with this article online at https://doi.org/10.1016/j.celrep.2017.10.074.

AUTHOR CONTRIBUTIONS

N.D., D.M.D., R.A.S., M.R.W., D.R.L., M.D., A.J.B.-W., A.W.T., and M.M., performed experiments. D.M.D., M.R.W., R.A.S., J.D.C., C.K.V., T.A.H., G.B., D.B., and M.M. designed experiments. M.M. wrote the manuscript and conceived the project.

ACKNOWLEDGMENTS

We would like to thank Dr. Gustavo de la Roza (Department of Pathology, SUNY Upstate Medical University) for his help and expert advice on the tumors. This work was partly supported by the National Institute of General Medical Sciences of the NIH (grant R01GM124256 to M.M.). The content is solely the responsibility of the authors and does not necessarily represent the official views of the NIH. This work was also supported by funds from SUNY Upstate Medical University, the Upstate Foundation, the One Square Mile of Hope Foundation, and the Carol M. Baldwin Breast Cancer Fund (D.B. and M.M.) and in part by the Urology Care Foundation Research Scholar Award Program and American Urological Association (M.M.).

Received: July 10, 2017
Revised: September 28, 2017
Accepted: October 19, 2017
Published: November 14, 2017

REFERENCES

Borowicz, S., Van Scoyk, M., Avasarala, S., Karuppusamy Rathinam, M.K., Tauler, J., Bikkavilli, R.K., and Winn, R.A. (2014). The soft agar colony formation assay. J. Vis. Exp. *92*, e51998.

Cancer Genome Atlas Research Network (2013). Comprehensive molecular characterization of clear cell renal cell carcinoma. Nature *499*, 43–49.

Chatterjee, A., Wang, L., Armstrong, D.L., and Rossie, S. (2010). Activated Rac1 GTPase translocates protein phosphatase 5 to the cell membrane and stimulates phosphatase activity in vitro. J. Biol. Chem. *285*, 3872–3882.

Cliff, M.J., Harris, R., Barford, D., Ladbury, J.E., and Williams, M.A. (2006). Conformational diversity in the TPR domain-mediated interaction of protein phosphatase 5 with Hsp90. Structure *14*, 415–426.

Clifford, S.C., Astuti, D., Hooper, L., Maxwell, P.H., Ratcliffe, P.J., and Maher, E.R. (2001). The pVHL-associated SCF ubiquitin ligase complex: molecular genetic analysis of elongin B and C, Rbx1 and HIF-1alpha in renal cell carcinoma. Oncogene *20*, 5067–5074.

Flotow, H., Graves, P.R., Wang, A.Q., Fiol, C.J., Roeske, R.W., and Roach, P.J. (1990). Phosphate groups as substrate determinants for casein kinase I action. J. Biol. Chem. *265*, 14264–14269.

Golden, T., Aragon, I.V., Rutland, B., Tucker, J.A., Shevde, L.A., Samant, R.S., Zhou, G., Amable, L., Skarra, D., and Honkanen, R.E. (2008a). Elevated levels of Ser/Thr protein phosphatase 5 (PP5) in human breast cancer. Biochim. Biophys. Acta *1782*, 259–270.

Golden, T., Swingle, M., and Honkanen, R.E. (2008b). The role of serine/threonine protein phosphatase type 5 (PP5) in the regulation of stress-induced signaling networks and cancer. Cancer Metastasis Rev. *27*, 169–178.

Gossage, L., Eisen, T., and Maher, E.R. (2015). VHL, the story of a tumour suppressor gene. Nat. Rev. Cancer *15*, 55–64.

Hasanov, E., Chen, G., Chowdhury, P., Weldon, J., Ding, Z., Jonasch, E., Sen, S., Walker, C.L., and Dere, R. (2017). Ubiquitination and regulation of AURKA identifies a hypoxia-independent E3 ligase activity of VHL. Oncogene *36*, 3450–3463.

Haslbeck, V., Drazic, A., Eckl, J.M., Alte, F., Helmuth, M., Popowicz, G., Schmidt, W., Braun, F., Weiwad, M., Fischer, G., et al. (2015a). Selective activators of protein phosphatase 5 target the auto-inhibitory mechanism. Biosci. Rep. *35*, e00210.

Haslbeck, V., Eckl, J.M., Drazic, A., Rutz, D.A., Lorenz, O.R., Zimmermann, K., Kriehuber, T., Lindemann, C., Madl, T., and Richter, K. (2015b). The activity of protein phosphatase 5 towards native clients is modulated by the middle- and C-terminal domains of Hsp90. Sci. Rep. *5*, 17058.

Iliopoulos, O., Kibel, A., Gray, S., and Kaelin, W.G., Jr. (1995). Tumour suppression by the human von Hippel-Lindau gene product. Nat. Med. *1*, 822–826.

Ivan, M., Kondo, K., Yang, H., Kim, W., Valiando, J., Ohh, M., Salic, A., Asara, J.M., Lane, W.S., and Kaelin, W.G., Jr. (2001). HIFalpha targeted for VHL-mediated destruction by proline hydroxylation: implications for O2 sensing. Science *292*, 464–468.

Jaakkola, P., Mole, D.R., Tian, Y.M., Wilson, M.I., Gielbert, J., Gaskell, S.J., von Kriegsheim, A., Hebestreit, H.F., Mukherji, M., Schofield, C.J., et al. (2001). Targeting of HIF-alpha to the von Hippel-Lindau ubiquitylation complex by O2-regulated prolyl hydroxylation. Science *292*, 468–472.

Kamura, T., Koepp, D.M., Conrad, M.N., Skowyra, D., Moreland, R.J., Iliopoulos, O., Lane, W.S., Kaelin, W.G., Jr., Elledge, S.J., Conaway, R.C., et al. (1999). Rbx1, a component of the VHL tumor suppressor complex and SCF ubiquitin ligase. Science *284*, 657–661.

Kamura, T., Sato, S., Iwai, K., Czyzyk-Krzeska, M., Conaway, R.C., and Conaway, J.W. (2000). Activation of HIF1alpha ubiquitination by a reconstituted von Hippel-Lindau (VHL) tumor suppressor complex. Proc. Natl. Acad. Sci. USA *97*, 10430–10435.

Kang, H., Sayner, S.L., Gross, K.L., Russell, L.C., and Chinkers, M. (2001). Identification of amino acids in the tetratricopeptide repeat and C-terminal domains of protein phosphatase 5 involved in autoinhibition and lipid activation. Biochemistry *40*, 10485–10490.

Kondo, K., Klco, J., Nakamura, E., Lechpammer, M., and Kaelin, W.G., Jr. (2002). Inhibition of HIF is necessary for tumor suppression by the von Hippel-Lindau protein. Cancer Cell *1*, 237–246.

Linehan, W.M. (2012). Genetic basis of kidney cancer: role of genomics for the development of disease-based therapeutics. Genome Res. *22*, 2089–2100.

Maxwell, P.H., Wiesener, M.S., Chang, G.W., Clifford, S.C., Vaux, E.C., Cockman, M.E., Wykoff, C.C., Pugh, C.W., Maher, E.R., and Ratcliffe, P.J. (1999). The tumour suppressor protein VHL targets hypoxia-inducible factors for oxygen-dependent proteolysis. Nature *399*, 271–275.

Mayer, M.P., and Le Breton, L. (2015). Hsp90: breaking the symmetry. Mol. Cell *58*, 8–20.

Mollapour, M., Tsutsumi, S., Donnelly, A.C., Beebe, K., Tokita, M.J., Lee, M.J., Lee, S., Morra, G., Bourboulia, D., Scroggins, B.T., et al. (2010). Swe1Wee1-dependent tyrosine phosphorylation of Hsp90 regulates distinct facets of chaperone function. Mol. Cell *37*, 333–343.

Oberoi, J., Dunn, D.M., Woodford, M.R., Mariotti, L., Schulman, J., Bourboulia, D., Mollapour, M., and Vaughan, C.K. (2016). Structural and functional basis of protein phosphatase 5 substrate specificity. Proc. Natl. Acad. Sci. USA *113*, 9009–9014.

Partch, C.L., Shields, K.F., Thompson, C.L., Selby, C.P., and Sancar, A. (2006). Posttranslational regulation of the mammalian circadian clock by cryptochrome and protein phosphatase 5. Proc. Natl. Acad. Sci. USA *103*, 10467–10472.

Ramsey, A.J., and Chinkers, M. (2002). Identification of potential physiological activators of protein phosphatase 5. Biochemistry *41*, 5625–5632.

Schittek, B., and Sinnberg, T. (2014). Biological functions of casein kinase 1 isoforms and putative roles in tumorigenesis. Mol. Cancer *13*, 231.

Shi, Y. (2009). Serine/threonine phosphatases: mechanism through structure. Cell *139*, 468–484.

Stebbins, C.E., Kaelin, W.G., Jr., and Pavletich, N.P. (1999). Structure of the VHL-ElonginC-ElonginB complex: implications for VHL tumor suppressor function. Science *284*, 455–461.

Vaughan, C.K., Mollapour, M., Smith, J.R., Truman, A., Hu, B., Good, V.M., Panaretou, B., Neckers, L., Clarke, P.A., Workman, P., et al. (2008). Hsp90-dependent activation of protein kinases is regulated by chaperone-targeted dephosphorylation of Cdc37. Mol. Cell *31*, 886–895.

Walton-Diaz, A., Khan, S., Bourboulia, D., Trepel, J.B., Neckers, L., and Mollapour, M. (2013). Contributions of co-chaperones and post-translational modifications towards Hsp90 drug sensitivity. Future Med. Chem. *5*, 1059–1071.

Wandinger, S.K., Suhre, M.H., Wegele, H., and Buchner, J. (2006). The phosphatase Ppt1 is a dedicated regulator of the molecular chaperone Hsp90. EMBO J. *25*, 367–376.

Wang, J., Zhu, J., Dong, M., Yu, H., Dai, X., and Li, K. (2015). Inhibition of protein phosphatase 5 (PP5) suppresses survival and growth of colorectal cancer cells. Biotechnol. Appl. Biochem. *62*, 621–627.

Woodford, M.R., Dunn, D., Miller, J.B., Jamal, S., Neckers, L., and Mollapour, M. (2016a). Impact of posttranslational modifications on the anticancer activity of Hsp90 inhibitors. Adv. Cancer Res. *129*, 31–50.

Woodford, M.R., Truman, A.W., Dunn, D.M., Jensen, S.M., Cotran, R., Bullard, R., Abouelleil, M., Beebe, K., Wolfgeher, D., Wierzbicki, S., et al. (2016b). Mps1 mediated phosphorylation of Hsp90 confers renal cell carcinoma sensitivity and selectivity to Hsp90 inhibitors. Cell Rep. *14*, 872–884.

Xu, W., Mollapour, M., Prodromou, C., Wang, S., Scroggins, B.T., Palchick, Z., Beebe, K., Siderius, M., Lee, M.J., Couvillon, A., et al. (2012). Dynamic tyrosine phosphorylation modulates cycling of the HSP90-P50(CDC37)-AHA1 chaperone machine. Mol. Cell *47*, 434–443.

Yang, J., Roe, S.M., Cliff, M.J., Williams, M.A., Ladbury, J.E., Cohen, P.T., and Barford, D. (2005). Molecular basis for TPR domain-mediated regulation of protein phosphatase 5. EMBO J. *24*, 1–10.

Zhou, G., Golden, T., Aragon, I.V., and Honkanen, R.E. (2004). Ser/Thr protein phosphatase 5 inactivates hypoxia-induced activation of an apoptosis signal-regulating kinase 1/MKK-4/JNK signaling cascade. J. Biol. Chem. *279*, 46595–46605.

Zuo, Z., Dean, N.M., and Honkanen, R.E. (1998). Serine/threonine protein phosphatase type 5 acts upstream of p53 to regulate the induction of p21(WAF1/Cip1) and mediate growth arrest. J. Biol. Chem. *273*, 12250–12258.

Zuo, Z., Urban, G., Scammell, J.G., Dean, N.M., McLean, T.K., Aragon, I., and Honkanen, R.E. (1999). Ser/Thr protein phosphatase type 5 (PP5) is a negative regulator of glucocorticoid receptor-mediated growth arrest. Biochemistry *38*, 8849–8857.